Tanzania Journal of Science 51(1): 152-168, 2025
ISSN 0856-1761, e-ISSN 2507-7961

Noise Subspace Channel Estimation Algorithm for OFDM Systems

Kwame S Ibwe
College of Information and Communication Technologies, University of Dar es Salaam
P. O. Box 33335, Dar es Salaam, Tanzania
Corresponding author e-mail: kwame.ibwe@gmail.com
Received 23 Oct 2024; Revised 6 Feb 2025; Accepted 20 March 25; Published 14 April 2025
https://dx.doi.org/10.4314/tjs.v51i1.11

Abstract

In this paper, a novel blind channel estimator for Orthogonal Frequency Division Multiplexing (OFDM) affected by unknown impulsive interference is proposed. Unlike conventional subspace-based methods, this approach combines noise subspace decomposition with eigenvalue filtering to enhance interference suppression and improve channel estimation accuracy. The proposed technique ensures precise estimation of the covariance matrix, which is critical for reliable channel state information (CSI) retrieval. Moreover, by incorporating the presence of virtual subcarriers, the method further refines the estimation of channel response. Simulation results demonstrate that the proposed algorithm significantly outperforms existing subspace-based estimators, particularly in highly time-varying wireless channels and low signal-to-noise ratio (SNR) conditions. These findings confirm the practical applicability of the method in next-generation wireless networks like 5G and beyond, where robust and accurate channel estimation is essential for maintaining communication reliability under adverse conditions.

Keywords: OFDM; Channel; Blind; Impulsive interference; Virtual subcarriers

Introduction

Orthogonal Frequency Division Multiplexing (OFDM) is recognized as a promising technology for broadband wireless networks (Rebouh et al. 2023). It has seen widespread adoption in wireless communications, including wireless LAN and digital video broadcasting-terrestrial (DVB-T) (Liu et al. 2022). In 2018, the Third Generation Partnership Project (3GPP) introduced 5G (fifth-generation mobile technology) as a new standard for cellular networks, replacing the previous standards of 3G, 4G, and 4G LTE (Chen et al. 2023). The goal of 5G was to establish a new set of standards for devices and applications compatible with its network. Like its predecessors, 5G uses radio waves for data transmission (Sarwar et al. 2023). However, due to advancements in latency, throughput, and bandwidth, 5G networks can achieve significantly faster download and upload speeds, enabling a broader range of applications (Jin et al. 2023). Theoretical data rates for 5G Release 17 reach up to 100 Gbps for downlink (DL) and 1 Gbps for uplink (UL) (Boodai et al. 2023).

OFDM is utilized in both DL and UL due to its capability to suppress frequency and time selectivity in channels (Ji et al. 2018, Manasa and Venugopal 2022). Channel estimates can be obtained using training symbols (Hussein et al. 2023) or through blind schemes (Bai and Bu 2004, Kawasaki and Matsumura 2022, Mehrabani et al. 2023). A popular class of blind channel estimators for OFDM systems involves subspace schemes (Li 2003), as explored in several studies (Alayyan et al. 2009, García-Naya et al. 2017, Rani and Singal 2023, Tang 2023). It is well established that OFDM systems are susceptible to various interferences (Amleh and Li 2008, Shafin et al. 2018). When the interference covariance can be reliably estimated at the receiver, pre-whitening can be applied before implementing subspace channel estimation (Wang et al. 2018). However, in the absence of sufficient information about the interference, pre-whitening cannot be performed, and subspace channel estimation becomes generally inaccurate (Mehrabani et al. 2023).

Interference reduction is a highly challenging issue (Basireddy and Moradi 2021), with the nature and characteristics of interference varying significantly across different applications (Schweizer et al. 2021). Additionally, interference characteristics change over time, making it difficult to develop a versatile algorithm effective in diverse environments. Furthermore, the objectives of an interference reduction system may depend on the specific context and application (Amleh and Li 2008, Hernandez et al. 2022, Mohammed and Hasan 2022). In signal processing and communication systems, implementing a robust interference reduction technique is crucial. Consequently, numerous researchers have focused on developing comprehensive noise reduction methods, leading to the proposal of various techniques (Hassanpour 2007, Li et al. 2022). The Wiener filter is known for its ability to reduce noise (interference) in a signal. However, this noise reduction is often accompanied by signal degradation. In other words, the Wiener filter is effective for noise reduction when the signal-to-noise ratio (SNR) is high (greater than 5 dB) (Dhanasekaran et al. 2022). When the SNR is below 5dB, using the Wiener filter may merely transform the noise into another form (Shamna and Amala 2020). Another recently introduced method for signal de-noising is time-frequency distribution (Li et al. 2022). This approach is notably effective in reducing noise even at low SNR. However, it is only applicable for bidirectional time-frequency distribution to reduce noise from time-series data, and it requires significant computational time to represent the signal in the time-frequency domain (Hussein et al. 2023, Mishra and Roy 2022). Subspace-based blind channel estimation techniques have been widely studied (Alayyan et al. 2009, Lalitha and Reddy 2022, Mishra and Roy 2022). These methods leverage the orthogonality of the signal and noise subspaces to estimate channel coefficients (Amleh and Li 2008, Wang et al. 2018). However, conventional subspace-based techniques struggle in scenarios where interference is impulsive and non-Gaussian, as they assume ideal noise characteristics (Mishra and Roy 2022). Additionally, these methods suffer from performance degradation in highly time-varying environments, where the covariance matrix estimation is affected by interference-induced distortions (Mehrabani et al. 2023, Rekik et al. 2024).

.

In this work, a new method is presented for reducing unknown interference in received signals using a combination of noise subspace decomposition and filtering of the eigenvalues associated with the vectors spanning the noise subspace. By accurately estimating and filtering the eigenvalues associated with noise components, the covariance matrix estimation process is improved, thereby enhancing the overall accuracy of channel estimation. A comparison of existing algorithms is conducted to evaluate channel estimation capability in terms of mean square error rate performance, assessed by the bit mean squared error to noise power ratio. These results are obtained using the MATLAB® simulation platform. To test the performance of the proposed method, flat and highly changing wireless channel environments are used, with channel models from Ling and Proakis (2017) and Mattera et al. (2021) for flat and highly changing channels respectively.

Materials and Methods

OFDM System Model

The analysis is based on Figure 1 and Figure 2 which show the OFDM discrete baseband transmitter and receiver with interference cancelation and channel estimation sections.

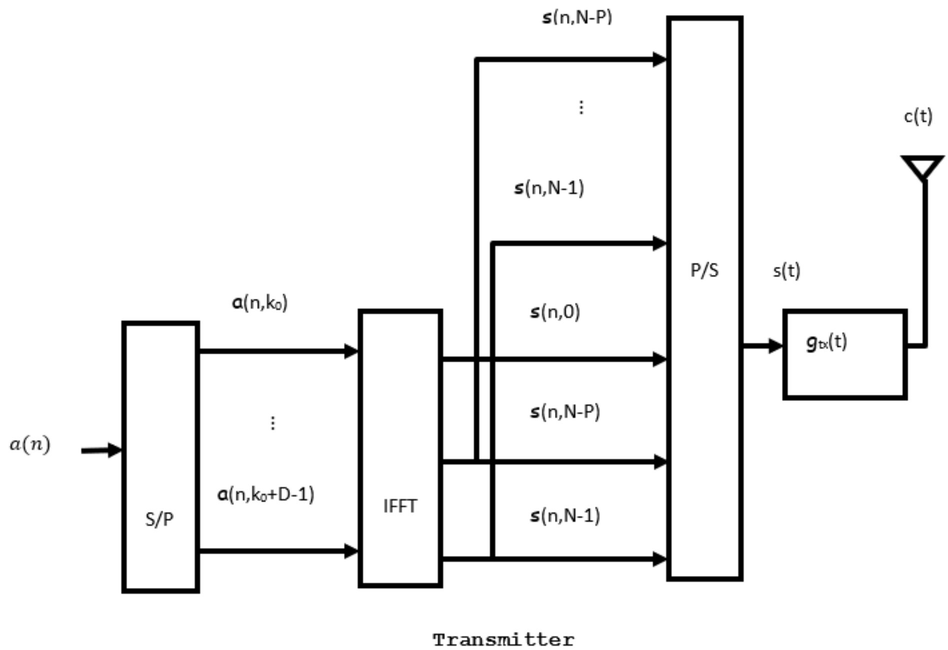

Figure 1: OFDM Baseband Discrete Time Transmitter

The symbols to be transmitted are given as

$$\boldsymbol{a}(n) = [a(n,k_0), a(n,k_1), \dots, \quad a(n,k_{N-1}+D-1)]^T \quad (1)$$

where D is the number of data subcarriers, N is the number of subcarriers, k_i is the kth subcarrier frequency, $n = \{\dots,-3,-2,-1,0,1,2,3,\dots\}$, $i =$ 0,1,2,…,N-1 and N-D the number of unmodulated subcarriers, referred to as virtual subcarriers (VCs). Let P be the length of cyclic prefix (CP), then for each OFDM symbol should be appended with the last P samples of itself after applying N-point IFFT operation on vector in equation (1). The resulting time domain signal is given as

$$\mathbf{s}(i) = [s(i,N-P), \dots, s(i,N-1), s(i,0), \dots \quad, s(i,N-1)]^T \quad (2)$$

The continuous time signal is pulse shaped by a transmit filter $g_{tx}(t)$ before transmission through the wireless channel

$$s(t) = \sum_{n=-\infty}^{\infty}\sum_{k=0}^{U-1} s(n, l\text{mod}N) g_{tx}[t-UT] \quad (3)$$

where T is the symbol duration, $U = n(N+P)+k$ and $= N-P+k$. However, equation (3) can simply be written as

$$s(t) = \sum_{U=-\infty}^{\infty} s(UT) g_{tx}(t-UT) \quad (4)$$

The signal is passed through channel of impulse response $h(t)$, corrupted by uncorrelated complex Gaussian noise $w(t)$ and filtered with receive filter $g_{rx}(t)$. The composite channel impulse response is given as

$$h(t) = g_{tx}(t) * c(t) * g_{rx}(t) \quad (5)$$

where (*) denote convolution operation.

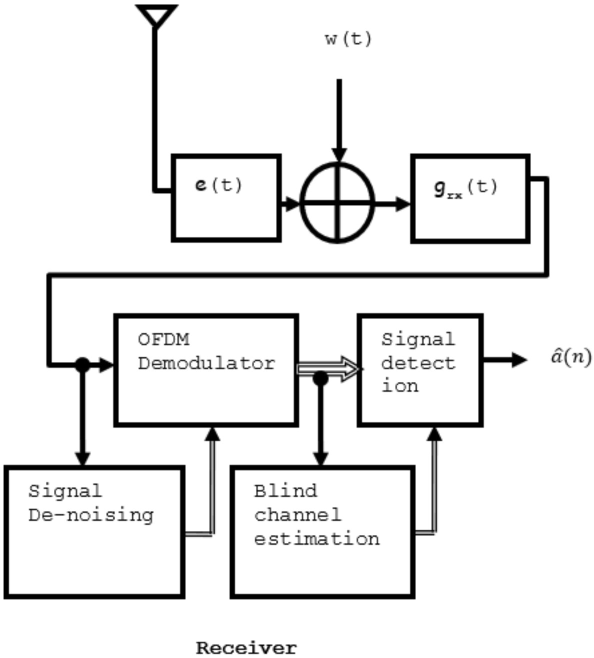

Figure 2: OFDM Baseband Discrete Time Receiver

The received signal *y(t)* is expressed as

$$y(t) = \sum_{U=-\infty}^{\infty} s(UT)h[t-UT] \quad + v(t) + e(t) \tag{6}$$

where $v(t) = w(t) * g_{rx}(t)$ and $e(t)$ are the filtered noise and impulsive interference respectively.

Assuming that channel has finite length of $L+1 \leq P$ coefficients, the sampled received signal at $t = mT_s$ is given as

$$y(mT_s) = \sum_{U=-\infty}^{\infty} s(UT)h[mT_s - UT] \quad + v(mT_s) + e(mT_s) \tag{7}$$

where $m = \{\dots, -3, -2, -1, 0, 1, 2, 3, \dots\}$ and T_s is the sampling time.

Blind Channel Estimator

In vector form the received signal is represented as

$$\mathbf{y}(n) = \mathbf{x}(\mathrm{n}) + \mathbf{e}(\mathrm{n}) + \mathbf{v}(n) \tag{8}$$

where $\mathbf{x}(\mathrm{n}) = \mathbf{H}\bar{\mathbf{F}}\mathbf{s}(\mathrm{n})$, $\mathbf{e}(\mathrm{n})$, $\mathbf{v}(\mathrm{n})$ are the transmit OFDM symbol, impulsive interference and Additive White Gaussian Noise (AWGN) respectively. The goal is to estimate $\mathbf{x}(\mathrm{n})$ from noisy $\mathbf{y}(\mathrm{n})$ and hence obtain accurate covariance matrix $\mathbf{R}_{yy}$.

The noisy signal $\mathbf{y}(\mathrm{n})$ can be represented by Hankel matrix for each OFDM symbol as

$$\mathbf{\Gamma} = \begin{bmatrix} \mathrm{y_n(1)} & \mathrm{y_n(2)} & \dots & \dots & \mathrm{y_n(K)} \\ \mathrm{y_n(2)} & \mathrm{y_n(3)} & \dots & \dots & \mathrm{y_n(K+1)} \\ \vdots & \vdots & \dots & \dots & \vdots \\ \vdots & \vdots & \dots & \dots & \vdots \\ \mathrm{y_n(L)} & \mathrm{y_n(L+1)} & \dots & \dots & \mathrm{y_n(N)} \end{bmatrix} \tag{9}$$

The Singular Value Decomposition (SVD) of matrix $\mathbf{\Gamma}$ with size P x Q is of the form

$$\mathbf{\Gamma} = \mathbf{U\Sigma V}^{\mathrm{T}} \tag{10}$$

where $\mathbf{U}_{\mathrm{P\,x\,r}}$ and $\mathbf{V}_{\mathrm{r\,x\,Q}}$ are orthogonal matrices and $\mathbf{\Sigma}$ is an r x r diagonal matrix of singular values with components $\sigma_{ij} = 0$ if $i \neq j$ and $\sigma_{ii} > 0$. Furthermore, it can be shown that $\sigma_{11} \geq \sigma_{22} \geq \sigma_{33} \geq 0$ (Forney 1975, Kawasaki and Matsumura 2022). The columns of the orthonomal matrices **U** and **V** are called the left and right singular values respectively. Hence, applying

Subspace Decomposition (SD) of the matrix $\mathbf{\Gamma}$ yields

$$\mathbf{\Gamma} = \mathbf{U\Sigma V}^{\mathrm{T}} = (\mathbf{U}_{\mathrm{s}} \quad \mathbf{U}_{\mathrm{n}}) \begin{bmatrix} \mathbf{\Sigma}_{\mathrm{s}} & 0 \\ 0 & \mathbf{\Sigma}_{\mathrm{n}} \end{bmatrix} \begin{pmatrix} \mathbf{V}_{\mathrm{s}}{}^{\mathrm{T}} \\ \mathbf{V}_{\mathrm{n}}{}^{\mathrm{T}} \end{pmatrix} \tag{11}$$

From equation 11 the signal and noise subspaces are separated. For each OFDM symbol the signal and noise subspace can now be expressed as

$$\mathbf{x}_{\mathrm{s}} = \mathbf{U}_{\mathrm{s}}\mathbf{U}_{\mathrm{s}}{}^{\mathrm{T}}\mathbf{\Gamma} = \mathbf{\Gamma V}_{\mathrm{s}}\mathbf{V}_{\mathrm{s}}{}^{\mathrm{T}} \tag{12}$$

$$\mathbf{w}_{n} = \mathbf{U}_{\mathrm{n}}\mathbf{U}_{\mathrm{n}}{}^{\mathrm{T}}\mathbf{\Gamma} = \mathbf{\Gamma V}_{\mathrm{n}}\mathbf{V}_{\mathrm{n}}{}^{\mathrm{T}} \tag{13}$$

where $\mathbf{\Sigma}_{\mathrm{s}}$ and $\mathbf{\Sigma}_{\mathrm{n}}$ represent the clean signal subspace and noise subspace respectively. The noise subspace is taken in this context to contain both noise and impulsive interference. As can be seen from (11) a threshold point in the $\mathbf{\Sigma}$ matrix has to be determined so that the separation of noise space from signal space can be done. In the work by (Hassanpour 2007), the threshold point is calculated by derivation of the curve in each point. In this work, the threshold point will be determined by SNR of the transmitted signal, since researches (Bröcker et al. 2002, Kirtland et al. 2023) show that noise subspace is mainly related to those singular values that are lower than the threshold point. This technique is termed here as SVD+SD technique.

After removing the impulsive interference effects on the received signal by SVD+SD technique the received signal can now be expressed as

$$y = \Xi a(n) + v(n) \tag{14}$$

It is shown in (Alayyan et al. 2009) that matrix Ξ has full column rank, if and only if $rank\left(H\left(e^{j\frac{2\pi}{N}i}\right)\right) = 1$ for all $i \in \{k\}_{k=k_0}^{k_0+D-1}$. The channel order is upper bounded by the length of CP, which is usually set to be greater than channel delay spread in practical OFDM systems. The autocorrelation matrix $R_{yy} = E\{y(n)y(n)^H\}$ of the interference-free received signal vector $y(n)$ is diagonalized through Eigen Value Decomposition (EVD) for noise and signal subspaces. The eigen vectors $\mathbf{U}$ are partitioned into the vectors $\mathbf{U}_s$ spanning the signal subspace $Span(U_s)$ and the vectors $\mathbf{U}_n$ spanning the noise subspace $Span(U_n)$ as

$$U = [U_s|U_n] = [u_1, u_2, \dots, u_D|u_{D+1}, u_{D+2}, \dots, u_{N+P-L}] \tag{15}$$

Since $Span(\Xi)$ and $Span(U_s)$ share the same D-dimensional space and are orthogonal to $Span\ (U_n)$, the following relationship holds

$$u_k{}^H\Xi = 0 \quad for\ all\ k \in \{n\}_{n=D+1}^{N+P-L} \tag{16}$$

Hence, the channel is estimated using $\hat{u}_k$ in (16) spanning $\widehat{U}_n$. In this case we can obtain the channel matrix estimate $\widehat{H}$ by minimizing a quadratic cost function $C(H)$ given as

$$C(H) = \sum_{k=D+1}^{N+P-L} \|u_k{}^H\Xi\|^2 \tag{17}$$

Partitioning the Eigen vector estimates $\hat{u}_k$ into *N*+*P*-*L* equal segments gives

$$\hat{u}_k = \begin{bmatrix} \hat{v}^k{}_1 \\ \hat{v}^k{}_2 \\ \vdots \\ \hat{v}^k{}_{N+P-L} \end{bmatrix} \tag{18}$$

Constructing the *L*+*1* x *N*+*P* matrix $\widehat{V}_k$ as

$$\widehat{V}_k = \begin{bmatrix} \hat{v}^k{}_1 & \dots & \hat{v}^k{}_{N+P-L} & 0 & \dots & 0 \\ 0 & \hat{v}^k{}_1 & \dots & \hat{v}^k{}_{N+P-L} & \dots & 0 \\ \vdots & 0 & \ddots & \vdots & \ddots & \vdots \\ 0 & \dots & 0 & \hat{v}^k{}_1 & \dots & \hat{v}^k{}_{N+P-L} \end{bmatrix} \tag{19}$$

and defining matrix Ψ as

$$\Psi \triangleq \sum_{k=D+1}^{N+P-L} \hat{V}_k (FF^H) \hat{V}_k{}^H \tag{20}$$

The cost function can now be written as

$$C(H) = h^H \Psi h \quad for \ \|h\|^2 = 1 \tag{21}$$

The estimated channel coefficients will now be obtained as

$$\hat{h} = [h_0 \ \ h_1 \ \ \ldots \ \ \ h_L] = \arg \ \min_{\|h\|^2=1} \ (h^H \Psi h) \tag{22}$$

The estimate of the channel response will be the Eigen vector associated with smallest Eigen value of Ψ. Since the direction and magnitude of h is not known a priori, there is inherent ambiguity in estimation. This ambiguity is cleared by a factor obtained by transmitting a few pilot symbols known to the receiver.

Experimental Results

Simulation and Analytical Parameters

In this section, the parameters for simulation analysis of the proposed channel estimation algorithm based on the noise subspace decomposition and filtering of Eigen values are presented. The proposed method is compared with the existing subspace (SS) methods presented in Wang et al. (2018) and Rekik et al. (2024). Table 1 shows the system and channel experimental conditions based on the IEEE 802.11ax standard (Mozaffariahrar et al. 2022) in the numerical experiments.

Table 1: Simulation and Experimental Conditions

Parameter	Value
OFDM symbol duration	$\frac{1}{300}$ ms
FFT-points N	512
Carrier frequency	2.4 GHz
Sampling interval T_s	72 µs
Modulation	QPSK
CP length T_g	$\frac{9}{128}$ T_s
Subcarrier mapping ($\boldsymbol{K} \leq \boldsymbol{N}$)	$-\frac{K}{2}, -\frac{K}{2}+1, \ldots\ldots, \frac{K}{2}-1$
Transmission bandwidth	5 MHz 10 MHz

The selection of the parameters in Table 1 is crucial for ensuring that the proposed method is evaluated under realistic and practical conditions. The carrier frequency of 2.4 GHz, FFT size, cyclic prefix, bandwidths and modulation scheme align with widely used wireless communication standards such as IEEE 802.11ax (Wi-Fi 6) (Mozaffariahrar et al. 2022) and LTE (Weerasinghe et al. 2020), making the findings applicable to modern broadband networks.

As a metric of the channel estimation accuracy, the mean square error (MSE) is defined as

$$MSE = \sqrt{\frac{1}{\kappa} \sum_{k=1}^{\kappa} \left\| \hat{h} - h \right\|^2} \tag{23}$$

where $\hat{h}_k$ denotes the *k-th* run estimate of the channel *h*. K denotes the number of runs and is chosen here to be 300. The signal symbols are drawn from QPSK constellation. The signal to noise power ration (SNR) of the channel is defined as

$$SNR_{dB} = 10log10\left(\frac{\mathrm{E}\{\|y_k\|^2\}}{\mathrm{E}\{\|v_k\|^2\}}\right) \tag{24}$$

In this work the bandwidth of transmission is assumed to be equal to the data rate. Therefore, the SNR defined in (24) can also be represented as

$$SNR_{dB} = 10log10\left(\frac{E_b}{N_0}\right) \tag{25}$$

where E_b and N_0 are energy per bit and noise power spectral density. For simulation, 5000 random symbols are generated and the system utilizes the IDFT transform with QPSK constellations. The channel is simulated as a L+1=51 tap FIR channel and is assumed that the channel taps are independent and identically distributed (i.i.d.) and correlate in time.

Results and Discussion

Simulation without Interference

The performance of the proposed blind channel estimator was evaluated and compared with the existing subspace (SS)-based methods presented in Wang et al. (2018) and Rekik et al. (2024). The comparison focused on the estimation capabilities of these methods in the absence of interference. The number of OFDM symbols was fixed to $K = 300$ and SNR is varied from 5 to 30 dB. The remaining system parameters were derived from IEEE 802.11ax standard (IEEE Computer Society LAN/MAN Standards Committee 2021). The channels under consideration were modeled as FIR filters with an order of L = 4. To thoroughly assess the estimator's performance, two extreme cases of channel coefficients were analyzed. In the first case, as shown in Table 2, the zeros of the channel were well separated. In the second case, as detailed in Table 3, the zeros of the channel were closely spaced. The results, illustrated in Figure 3 for the well-separated zeros scenario (corresponding to Table 2) and in Figure 4 for the closely spaced zeros scenario (corresponding to Table 3), demonstrate a clear performance advantage of the proposed estimator over the existing SS-based methods.

Table 2: Channel with well-spaced zeros

l	0	1	2	3	4
$h(l)$	0.1-0.1i	0.5-0.5i	0.9-0.9i	1.2-1.2i	1.5-1.5i

Table 3: Channel with closely spaced zeros

l	0	1	2	3	4
$h(l)$	0.2-0.2i	0.3-0.3i	0.4-0.4i	0.5-0.5i	0.6-0.6i

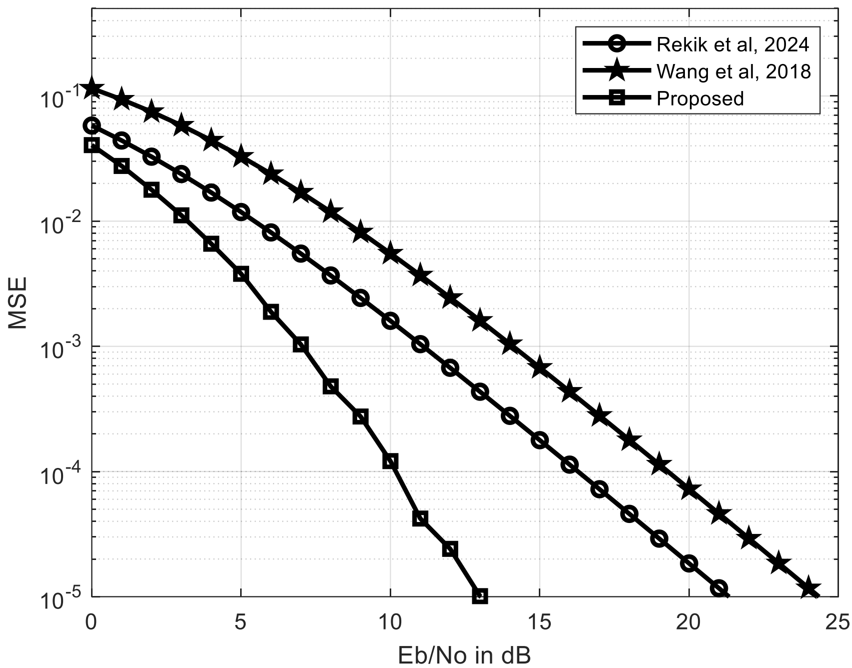

Figure 3: MSE vs SNR for proposed and existing SS-based methods for channel with well spaced zeros without interference.

.

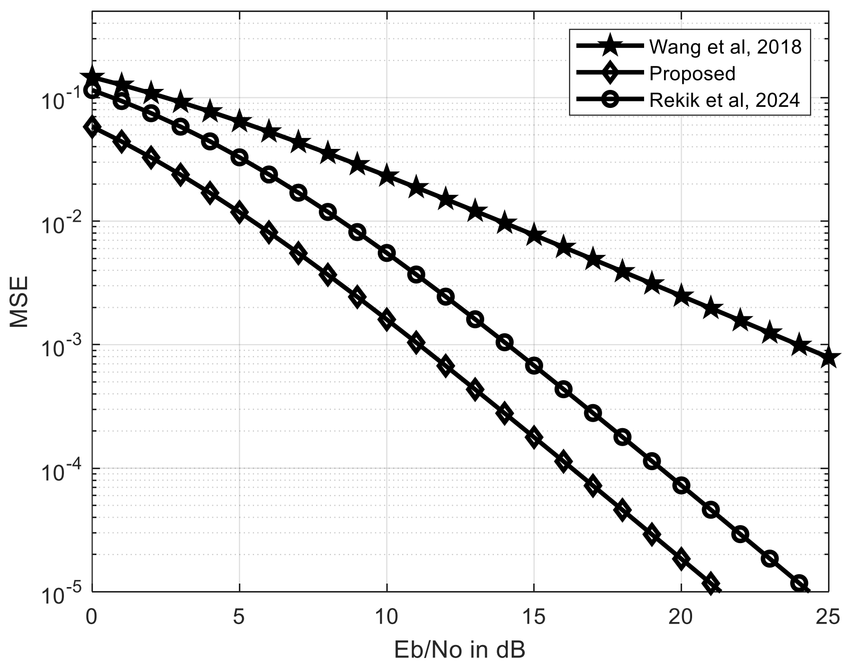

Figure 4: MSE vs SNR for proposed and existing SS-based methods for channel with closely spaced zeros without interference

Specifically, the proposed method exhibits superior performance across a wide range of SNR values in both channel conditions. A notable observation is that when the channel zeros are closely spaced, the performance of existing methods significantly deteriorates at low SNR levels. This is particularly evident in Figure 4, where the existing methods struggle to provide accurate channel estimation under these challenging conditions. In contrast, the proposed estimator maintains robust performance, highlighting its effectiveness in handling doubly dispersive channels with poorly spaced zeros.

Simulation with Interference

In addition to evaluating the performance of the proposed blind channel estimator in the absence of interference, the proposed method was assessed for its robustness in the presence of random interference. Using the same system and channel parameters as in the initial simulation setup, the experiment was repeated with random interference added to the received signal, as illustrated in Figure 5.The interference was modeled as a series of randomly spaced pulses with infinitesimal duration, simulating a realistic scenario where impulsive noise can severely affect signal quality. The results, depicted in Figures 6 and 7, demonstrate the performance of the proposed method compared to existing SS-based methods under these challenging conditions. Specifically, Figure 6 corresponds to the scenario with well-separated zeros (similar to Table 2), while Figure 7 pertains to the scenario with closely spaced zeros (similar to Table 3). The proposed method consistently outperformed the existing methods by a significant margin of 5 dB across various SNR levels. This notable improvement underscores the robustness of the proposed estimator in mitigating the effects of random interference. In the presence of random interference, the existing SS-based methods exhibited considerable degradation in performance, especially at lower SNR levels. This is observed in the closely spaced zeros scenario (Figure 7), where the existing methods could not maintain accurate channel estimation. In contrast, the proposed method demonstrated remarkable resilience, maintaining high estimation accuracy even in the presence of interference.

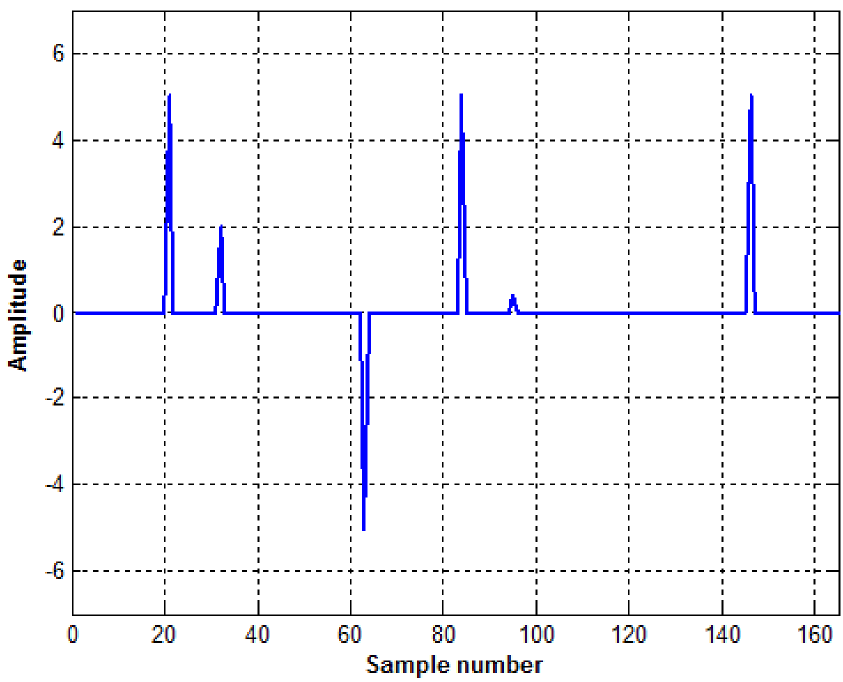

Figure 5: Random Generated Interference Impulses

.

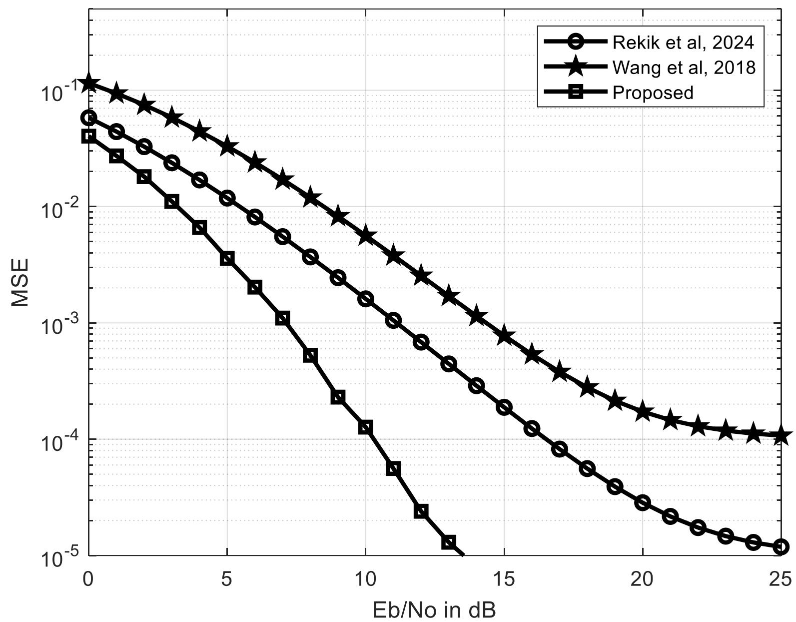

Figure 6:MSE vs SNR for proposed and existing SS-based methods for channel with well-spaced zeros with interference

.

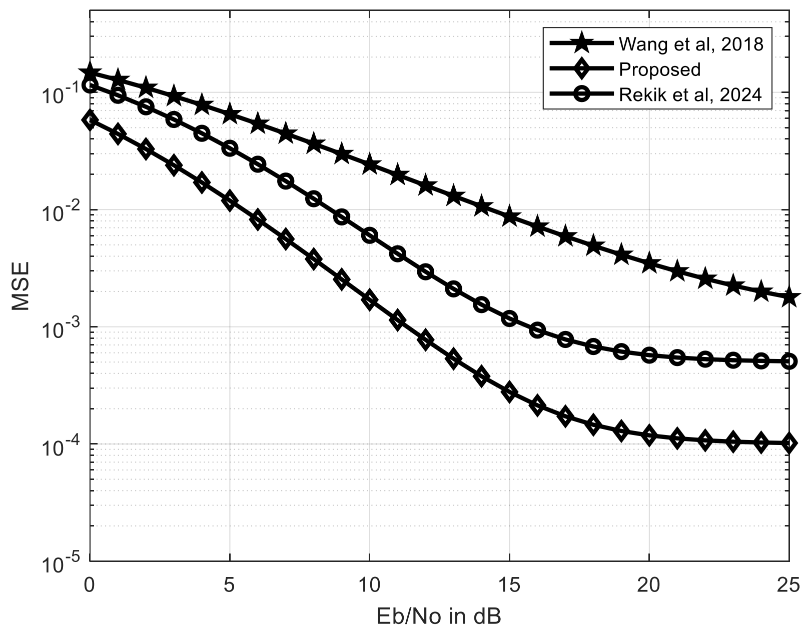

Figure 7: MSE vs SNR for proposed and existing SS-based methods for channel with closely spaced zeros with interference

The convergence behavior of the proposed estimator and the existing subspace (SS)-based methods was analyzed under the conditions specified in Table 2 (well-spaced zeros) and Table 3 (closely spaced zeros). Figures 8 and 9 illustrate the convergence performance of both estimators as a function of the number of OFDM symbols at an SNR of 10 dB. Convergence is a critical metric as it indicates how quickly an estimator can achieve reliable channel estimation with an increasing number of OFDM symbols. A faster convergence implies that the estimator requires fewer symbols to accurately identify the channel characteristics, which is particularly advantageous in dynamic communication environments. As depicted in Figures 8 and 9, the performance of both the proposed and existing estimators improves with an increasing number of OFDM symbols.

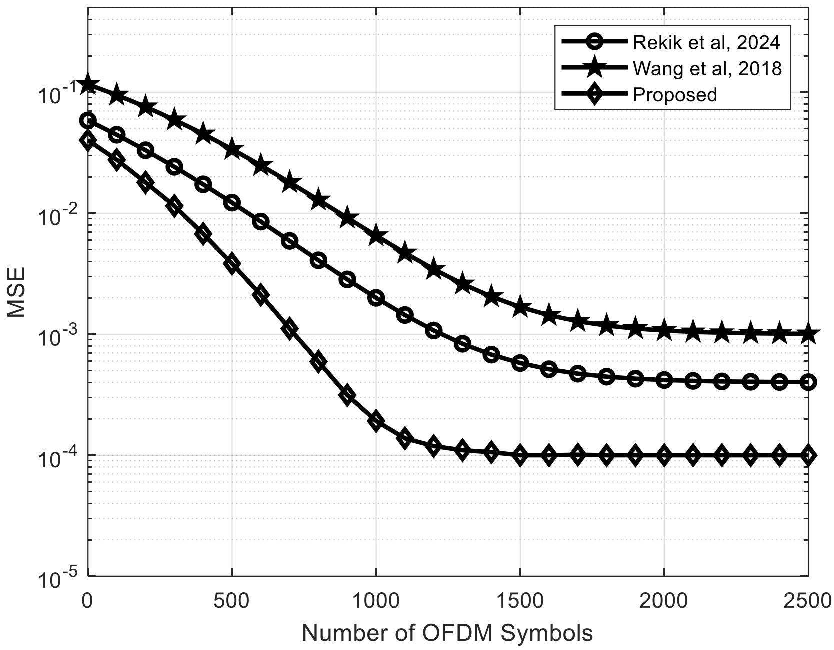

Figure 8: Convergence of proposed and existing SS-based methods for channel with well-spaced zeros with interference

.

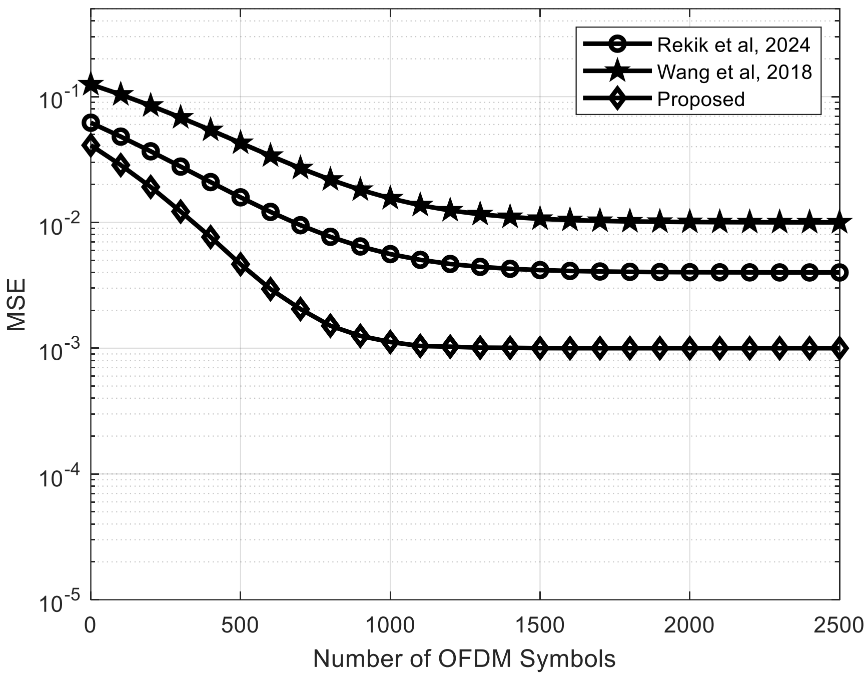

Figure 9: Convergence of proposed and existing SS-based methods for channel with closely spaced zeros with interference

However, a significant difference in convergence rates is observed between the two methods. For the scenario with well-spaced zeros (Figure 8), the proposed method demonstrates rapid convergence, achieving reliable channel identification with less than 1000 OFDM symbols. In contrast, the existing SS-based methods require at least 1500 OFDM symbols to achieve comparable performance in flat fading channels. This faster convergence of the proposed method highlights its efficiency and effectiveness in estimating channel coefficients under favorable conditions. In the more challenging scenario with closely spaced zeros (Figure 9), the proposed method continues to exhibit superior performance. It converges with at least 1000 OFDM symbols, while the existing methods require around 2000 OFDM symbols to reach similar levels of accuracy in highly dispersive channels. This demonstrates the robustness of the proposed method in handling complex channel conditions, where the zeros of the channel are closely spaced, and the channel exhibits significant variation.

For fair comparison between proposed and existing subspace based OFDM channel estimation schemes, the computational complexity is presented in Table 4. The complexity in this study is defined as of the number of multiplications, additions, matrix inversions and computational resources needed to complete each iteration. N is the number of OFDM subcarriers, Γ^{-1} is the inverse of Hankel matrix, P is the number of rows in the Hankel matrix, Q is the number of columns in the Hankel matrix and $O(.)$ is the computational complexity order.

Table 4: Computational Complexity of Subspace-Based Channel Estimation Schemes

Scheme	**Complexity**
Wang et al., 2018	$\mathcal{O}(N^3).\Gamma^{-1}\mathcal{O}(N^2)$
Rekik et al., 2024	$(\mathcal{O}(N^3) + \mathcal{O}(PQ^2)).\Gamma^{-1}$
Proposed Method	$\mathcal{O}(PQ^2)+ \mathcal{O}(Q^2).\Gamma+ \mathcal{O}(N^2)$

The computational complexity analysis highlights that conventional subspace-based methods presented in Wang et al. (2018) and Rekik et al. (2024), rely on matrix inversion and full eigenvalue decomposition (EVD), leading to a high complexity of $(\mathcal{O}(N^3)$. While Rekik et al. (2024) integrates singular value decomposition (SVD) to improve noise subspace estimation, it still incurs significant computational overhead. In contrast, the proposed SVD+SD based method achieves a more balanced trade-off between accuracy and efficiency by banking on noise subspace decomposition and eigenvalue filtering, reducing the dependency on high-complexity matrix inversion. Despite the added cost of $\mathcal{O}(PQ^2)$ for SVD and $\mathcal{O}(Q^2)$ for EVD, the proposed method improves convergence speed and estimation accuracy, ultimately requiring fewer OFDM symbols to achieve reliable channel estimation. This makes it more suitable for high-mobility and interference-prone environments, such as 5G and beyond systems.

Figures 10 and 11 present the overall bit error rate (BER) performance of the proposed method compared to existing subspace (SS)-based methods, as a function of SNR, under the channel settings described in Table 2 and Table 3, respectively. In Figure 10, where the zeros of the channel are well-spaced, the proposed method achieves an impressive BER of 10^{-6} at an SNR of 15 dB. In comparison, the methods by Rekik et al. (2024) and Wang et al. (2018) achieve the same BER at significantly higher SNRs of 22 dB and 27 dB, respectively. This substantial difference highlights the energy efficiency of the proposed method, as lower SNR requirements translate to reduced power consumption. In Figure 11, the BER performance is assessed under the channel settings of Table 3, where the zeros of the channel are closely spaced. Although the performance of the proposed method slightly deteriorates due to the more challenging channel characteristics, it still outperforms the existing methods. The proposed method achieves a BER of 10^{-6} at an SNR of 17 dB, whereas the methods by Rekik et al. (2024) and Wang et al. (2018) require SNRs of 23 dB and 28 dB, respectively, to reach the same BER level. This demonstrates the proposed method's robustness and efficiency even in complex and highly dispersive channel conditions.

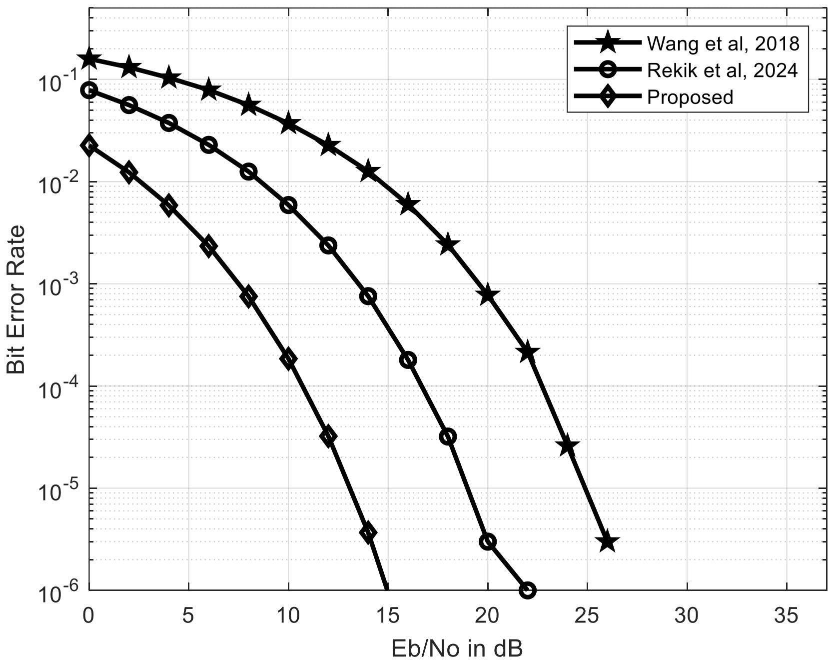

Figure 10: BER vs SNR performance of proposed and existing SS-based methods for channel with well-spaced zeros with interference

.

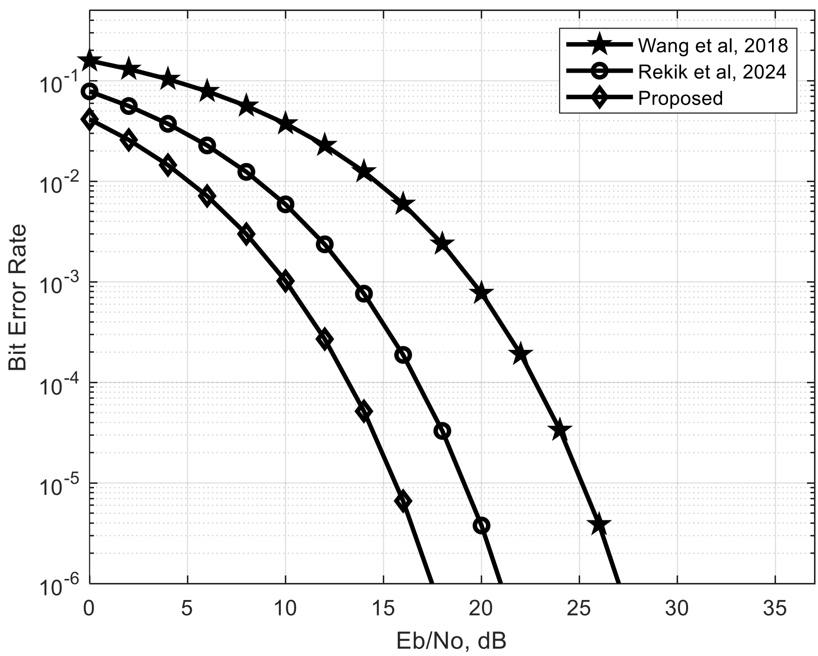

Figure 11:BER vs SNR of proposed and existing SS-based methods for channel with closely spaced zeros with interference

The results presented in this section highlight the effectiveness of the proposed channel estimation method under various wireless channel conditions. The selection of simulation parameters, including carrier frequency, bandwidth, and modulation scheme, is based on widely used communication standards such as IEEE 802.11ax and LTE, ensuring that the findings are applicable to practical broadband networks. The observed improvements in MSE, BER, and convergence behavior confirm that the proposed method provides robust and efficient channel estimation, particularly in environments affected by impulsive interference and high mobility. These insights are critical for the development of next-generation OFDM-based wireless systems, where reliable and low-complexity channel estimation is essential for maintaining communication quality.

Conclusion

In this paper, a blind channel estimator for Orthogonal Frequency Division Multiplexing (OFDM) in the presence of unknown impulsive interferences was presented. The impulsive interference reduction in received signal was done using SVD+SD technique. The technique used a combination of noise subspace decomposition and filtering of the Eigen values associated with the vectors spanning the noise subspace. Then the improved subspace method which utilizes the presence of virtual subcarriers was applied to the estimated covariance matrix to approximate the channel. The key to accurate estimation of the channel coefficients was accurate estimation of autocorrelation matrix of received. The proposed channel estimator was able to outperform the existing blind estimators with average of 5dB at error rate of 10^{-2} for badly spaced channel zeros. Furthermore, the complexity of the proposed scheme can be adjusted by varying the number of considered interference eigenvalues in the SVD+SD technique, however, at the cost of estimation accuracy and consequently performance. These findings have significant implications for the design of OFDM systems operating in environments with impulsive interference and doubly dispersive channels. The ability to maintain high estimation accuracy under such conditions can lead to more reliable and efficient communication systems. Future work could explore the application of the proposed estimator in different OFDM standards and its performance in real-world scenarios. Additionally, further optimization of the method to reduce computational complexity while maintaining estimation accuracy would be a valuable direction for research.

References

Alayyan FO, Shubair RM, Zoubir AM and Leung YH 2009 Blind channel identification and equalisation in OFDM using subspace-based methods. *J. Commun*. 4(7): 472-484.

Amleh K and Li H 2008 Blind-channel estimation and interference suppression for single-carrier and multicarrier block transmission systems. *IEEE Trans. Vehicular Tech*. 57(5): 2779-2791.

Bai W and Bu Z 2004 Subspace based channel estimation in MIMO-OFDM systems. *IEEE Vehicular Tech. Conf*. 2(1): 598-602.

Basireddy A and Moradi H 2021 OFDM Waveform Design for Interference Resistant Automotive Radars. *IEEE Sensors J.*. 21(14): 15670-15678.

Boodai J, Alqahtani A and Frikha M 2023 Review of Physical Layer Security in 5G Wireless Networks. *Appl. Sci*. 13(12). 7277.

Bröcker J, Parlitz U and OgorzaŁek M 2002 Nonlinear noise reduction. *Proc. of the IEEE*. 90(5): 898-918.

Chen W, Lin X, Lee J, Toskala A, Sun S, Chiasserini CF and Liu L 2023 5G-Advanced Toward 6G: Past, Present, and Future. *IEEE J. Select. Areas Commun*. 41(6): 1592 - 1619.

Forney GD 1975 Minimal bases of rational vector spaces, with applications to multivariable linear systems. *SIAM J. Control*. 13(3): 493-520.

García-Naya JA, Heath R, Kaltenberger F, Rupp M and Vía J 2017 Experimental evaluation in wireless communications. *J. Wireless Commun. Network*. 59(1). 1-12.

Hassanpour H 2007 Improved SVD-based technique for enhancing the time-frequency representation of signals. *IEEE Int. Symp. Circuits Syst*.1819-1822.

Hernandez FJ, Omri A and Oligeri G 2022 A noise reduction scheme for OFDM NB-PLC systems. *Adv. Electr. Eng. Electron. Energy*. 2(7).100043.

Hussein W, Audah K, Noordin NK, Kraiem H, Flah A, Fadlee M and Ismail A 2023 Least Square Estimation-Based Different Fast Fading Channel Models in MIMO-OFDM Systems. *IEEE Trans. Electr. Energy Syst*. 2023(1):1-23.

IEEE Computer Society LAN/MAN Standards Committee 2021 *Part 11: Wireless LAN Medium Access Control (MAC) and Physical Layer (PHY) Specifications, Amendment 1: Enhancements for High-Efficiency WLAN. IEEE Std 802.11ax-2021*.

Ji H, Park S, Yeo J, Kim Y, Lee J and Shim B 2018 Ultra-Reliable and Low-Latency Communications in 5G Downlink: Physical Layer Aspects. *IEEE Wireless Commun*. 25(3): 124-130.

Jin H, Liu K, Zhang M, Zhang L, Lee G, Farag EN, Zhu D, Onggosanusi E, Shafi M and Tataria H 2023 Massive MIMO Evolution Toward 3GPP Release 18. *IEEE J. Select. Areas Commun*. 41(6). 1635-1654.

Kawasaki H and Matsumura T 2022 Semi-Blind Channel Estimation by Subspace Method for Orthogonal Precoded OFDM Systems. *IEEE Ann. Int. Symp. Personal, Indoor Mobile Radio Commun*. 451–456.

Kirtland A, Botvinick-Greenhouse J, DeBrito M, Osborne M, Johnson C, Martin RS, Araki SJ and Eckhardt DQ 2023 An Unstructured Mesh Approach to Nonlinear Noise Reduction for Coupled Systems. *SIAM J. Appl. Dynam. Syst*. 22(4). 2927-2944.

Lalitha A and Reddy GH 2022 Blind Channel Estimation Using Enhanced Independent Component Analysis for MIMO-OFDM System. *Int. Intel. Eng. Syst*. 15(5). 25-34.

Li H 2003 Blind channel estimation for multicarrier systems with narrowband interference suppression. *IEEE Commun. Lett*. 7(7). 326-328.

Li JP, Li ML, Yang T and Xue P 2022 Low-complexity Wiener filter channel estimation algorithm in massive MIMO-OFDM system. *J. Jilin Uni*. 52(1). 211-218.

Ling F and Proakis J 2017 Synchronization in Digital Communication Systems. 2nd ed, Cambridge University Press, Cambridge.

Liu D, Luo Y, Li Y, Wang Z, Li Z, Zhang Q, Zhang J and Li Y 2022 An LDPC Encoder Architecture with Up to 47.5 Gbps Throughput for DVB-S2/S2X Standards. *IEEE Access*. 10(1). 19022-19032.

Manasa BMR and Venugopal P 2022 A systematic literature review on channel estimation in MIMO-OFDM system: Performance analysis and future direction. *J. Opt. Commun*. 45(3). 589-614.

Mattera D, Tanda M and Bellanger M 2021 Comparing the performance of OFDM and FBMC multicarrier systems in doubly-dispersive wireless channels. *Signal Process*. 179(10):107818.

Mehrabani MR, Abolhassani B, Haddadi F and Tellambura C 2023 Second-Order Statistics-Aided Channel Estimation for Multipath Massive MIMO-OFDM Systems. *IEEE Access*. 11. 21921-21933.

Mishra S and Roy JS 2022 Blind channel estimation for ofdm systems using sparse adaptive signal processing algorithms. *Telecom. Radio Eng*. 81(10). 1-15.

Mohammed ML and Hasan FS 2022 Design and performance analysis of frequency hopping OFDM based noise reduction DCSK system. *Bull. Electr. Eng. Inform*. 11(3). 1438-1448.

Mozaffariahrar E, Theoleyre F, and Menth M 2022 A Survey of Wi-Fi 6: Technologies, Advances, and Challenges. *Future Internet*. 14(10). 293.

Rani M and Singal P 2023 Perceptron for channel estimation and signal detection in OFDM systems. *J. Optics*. 52(1). 69-76.

Rebouh D, Djebbar AB and Besseghier M 2023 Blind joint CFO and STO estimation for FBMC/OQAM systems. *IEEE Commun. Lett.* 27(9). 2422-2426.

Rekik O, Aliyu KN, Tuan BM, Abed-Meraim K and Trung NL 2024 Fast Subspace-based Blind and Semi-Blind Channel Estimation for MIMO-OFDM Systems. *IEEE Trans. Wireless Commun*. 23(8). 10247-10257.

Dhanasekaran S, Palanisamy SK, Hajjej F, Khalaf OI, Abdulsahib GM and S R 2022

Discrete Fourier Transform with Denoise Model Based Least Square Wiener Channel Estimator for Channel Estimation in MIMO-OFDM. *Entropy*. 24(11). 1601.

Sarwar MS, Ahmad M and Shin SY 2023 Subcarrier Index Modulation for Spectral Efficient Frequency Division Multiplexing in Multi-Input Multi-Output Channels. *IEEE Trans. Vehicle. Tech*. 72(2). 2678-2683.

Schweizer B, Knill C, Werbunat D, Stephany S and Waldschmidt C 2021 Mutual Interference of Automotive OFDM Radars-Analysis and Countermeasures. *IEEE J. Microwaves*. 1(4). 950-961.

Shafin R, Liu L, Ashdown J, Matyjas J and Zhang J 2018 On the channel estimation of multi-cell massive FD-MIMO systems. *IEEE Int. Conf. Commun*. 1-6.

Shamna AR and Amala Shanthi S 2020 An approach for reduce distortion and improve system performance of MIMO-OFDM using wiener hammerstein equalizer. *J. Adv. Res. Dynam.Control Syst*. 12(4). 1-15.

Tang Z 2023 OFDM communication system based on FPGA. *Proc. Conf. Commun. Technol. Comput. Sci.* 666-670.

Wang H, Liao J, Xu L and Wang X 2018 Blind channel estimation for FBMC/OQAM systems based on subspace approach. *Information* . 9(3). 58.

Weerasinghe TN, Balapuwaduge IAM and Li FY 2020 Priority-based initial access for URLLC traffic in massive IoT networks: Schemes and performance analysis. *Comput. Networks*. 178(1). 107360.